Journal of Analytical and Applied Pyrolysis 172 (2023) 105993

Contents lists available at ScienceDirect

Journal of Analytical and Applied Pyrolysis

journal homepage: www.elsevier.com/locate/jaap

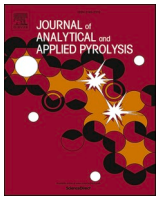

Tandem mass spectrometry enhances the performances of pyrolysis-gas chromatography-mass spectrometry for microplastic quantification

Magali Albignac [a], Tiago de Oliveira [a], Louisa Landebrit [a], Sébastien Miquel [b], Benoit Auguin [c], Eric Leroy [d], Emmanuelle Maria [a], Anne Françoise Mingotaud [a], Alexandra ter Halle [a,*]

[a] CNRS, Université Toulouse III, Laboratoire des Interactions Moléculaires et Réactivité Chimique et Photochimique (IMRCP), UMR 5623 Toulouse, France
[b] Thermo Fisher, Courtaboeuf, France
[c] Quad Service, Achères, France
[d] CNRS, Université Toulouse III, Institut de Chimie de Toulouse (ICT), UAR 2599 Toulouse, France

ARTICLE INFO

Keywords:
Plastic
Polymer
Nanoplastic
Py-gc-ms
Plastic debris

ABSTRACT

The ability of pyrolysis gas chromatography—mass spectrometry to quantify microplastics has been demonstrated; this study aims to provide a robust method using tandem mass spectrometry in order to gain in sensitivity and selectivity. The preparation of homogeneous and repeatable solid standards allowed us to perform an external calibration for six polymers in the nanogram range. Relevant indicator compounds were selected for each targeted polymer, and multiple reaction monitoring optimization was undertaken. The linearity, standard deviation and overall sensitivity were examined. After optimization, the detection limit was 15–70 ng according to the polymer. Interferences between polymers were examined, and we demonstrated that tandem mass spectrometry was necessary for the unequivocal detection of some polymers such as polyethylene and polypropylene. The method was applied to analyze the plastic particle content in bottled water. Only polyethylene terephthalate chemical compound was quantified at 42 ng.L^{-1}. For future development, the use of internal standards will increase the method precision. It will also be important to better understand the interferences with the matrix in complex samples and the potential impact of weathering on the polymer pyrolytic response.

1. Introduction

Recent studies have shown that the natural environment [1], our food [2] and beverages [3] are contaminated with small plastic particles. Masses of plastic debris accumulate in the environment due to a combination of high production, poor development of waste collection infrastructures and low recycling volumes [4,5]. Environmental factors such as sunlight or mechanical stress promote plastic debris fragmentation and erosion into very small particles [6]. The fate and route of transportation of microplastics are poorly understood in relations to the risks associated with ecosystem exposure or human health. This lack of awareness is mainly related to the need to achieve fast and reliable methods to analyze microplastics in complex samples.

Several challenges arise with respect to the analysis of microplastics in environmental matrices. Polymers in the samples have usually undergone weathering and profound structural modifications, which makes sample preparation and identification challenging [7,8]. The task is even more challenging with smaller microplastics sizes to finally reach a knowledge and technology gap below 150 μm [9]. Very important analytical progress was achieved with spectroscopic measurements. Breakthrough methods have emerged, e.g., with the development of automated particle identification and data processing, which greatly reduced the time analysis and conferred robustness to the methods [10,11]. In parallel, pyrolysis−gas chromatography—mass spectrometry (Py-GC—MS) appears to be a novel promising technique [12–14]. One of its interesting aspects is that it does not have size limitations, which offers the possibility to analyze nanoplastics [15,16]. The other interesting potential in using Py-GC-MS is to overcome extensive sample preparation processes [2,17,18]. Beyond detection, quantification was also performed [2,18–22]. Quantification consists of selecting one molecule among many decomposition products after pyrolysis to proceed to the quantification; this specific molecule is called the indicator compound. Most described methods monitor the indicator compounds using a simple quadrupole by ion extraction after full scan recording [19,23] or by single ion monitoring (SIM) [2,18,20,21]. The potentiality of mass spectrometry was scarcely explored even if the gain from using

* Corresponding author.
E-mail address: alexandra.ter-halle@cnrs.fr (A. ter Halle).

https://doi.org/10.1016/j.jaap.2023.105993
Received 16 December 2022; Received in revised form 24 April 2023; Accepted 2 May 2023
Available online 8 May 2023

high-resolution mass spectrometry was recently proposed and the advantages were noticeable [17,24]. The aim of the study is to use tandem mass spectrometry (Py-GC-MS/MS) in order to improve the sensitivity and selectivity of the analysis with the achievement of lower limits of quantification. Since very low detection limits were reached, we paid close attention to quality assurance and quality control to minimize contamination during sample preparation and handling. For completion, the method was applied to detect and quantify microplastics in bottled water.

2. Materials and methods

2.1. Chemicals

The polymers selected as external standards are high-density polyethylene (PE), poly(methyl methacrylate) (PMMA), polyethylene terephthalate (PET), polycarbonate (PC), polystyrene (PS), and polypropylene (PP), and their characteristics are listed in Table SI1. The selected indicator compound standards are methylmethacrylate (MeMeta), 1,13 tetradecadiene (C14D), 1,14 pentadecadiene (C15D), dimethylterphtalate (DMeTPh), 2,2-bis(4'-methoxy-phenyl)propane (BPAMe), 2,4-dimethylhept-1-ene (DMC7), 2,4,6,8-tetramethyl-1-undecene (TeMC11), 2,4,6-Triphenyl-1-hexene (SSS) and 2,4-diphenyl-1-butene (SS), as listed in Table SI2. Tetramethylammonium hydroxide pentahydrate (TMAH) was purchased from Sigma-Aldrich with a minimum purity of 97%. For the GC-MS/MS optimization, the indicator compounds were dissolved in dichloromethane (VWR, Pennsylvania, USA). Absolute ethanol (VWR, Pennsylvania, USA) was used to clean the materials. Ultra-pure water (18.2 MΩ cm) was obtained from a Milli-Q filtration unit (Merck Millipore, MA, USA).

2.2. Quality assurance and quality control (QA and QC)

Koealmans et al. recently stressed the need for stricter QA when analyzing microplastics in water samples [3]. Their recommendations were considered, and special care was taken to minimize contamination. Cotton lab clothes were adopted to avoid any risk of contamination from synthetic materials. The use of cotton masks was preferred to synthetic masks, since the experiments were conducted during covid19 pandemic. Sample handling was performed in a clean air laboratory under a daily cleaned hood. Sample preparation was only performed with glass or metal equipment. All glassware was pretreated by calcination at 550 °C: 1.5 h of heating from room temperature to 550 °C, 1.5 h of holding at this temperature and slow cooling overnight using an LV 5/11 furnace from Nabertherm®. The glass fiber filters (GF/F, porosity 0.7 μm, Whatman®) were prepared after an optimized calcination to remove any trace polymer and consisted of heating from room temperature to 500 °C at a rate of 80 °C/hour with a hold of 30 h at 500 °C in the same furnace. The furnace programming optimization was realized by analyzing the filter by Py-GC-MS/MS; especially the remaining signal of PE was monitored as it was relatively initially important in the filters. The cells for cryogenic grinding (SPEX® SamplePrep 6775 Freezer/Mill cryogenic Grinder, Delta Labo, France) were always cleaned before any use: first by calcination and subsequently by washing with ethanol and kimtex tissue (high-performance wiper 7624 from Kimberly-Clark Professional®). The use of an appropriate methylation agent was optimized regarding contamination introduction. The pyrolysis quartz tubes (from Quad Service, France) were freshly pre-calcined at 1000 °C. The quartz tubes were weighed before and after adding samples using a Micro Balance from Sartorius (MCE2^{25}P–^{2}S00-A Cubis®-II Semi) with a sensitivity of 0.01 mg. The samples were placed in an inox sample holder under a glass bell to dry for 1 h before being placed into the pyrolysis autosampler.

2.3. Preparation of external calibration standard

All polymers were first cryo-milled using the SPEX® cryogenic Grinder. The cryo-milling program was as follows: precool 2 min; run 1 min; cool 2 min; cycles 15; cps 15. Then, the ground polymers were mixed with an inert glass fiber matrix. This inert matrix was prepared from glass fiber filters that were cryo-milled (precooled for 1 min; cooled for 1 min; cycled 6; cps 15) and calcined. The standards were first prepared at concentrations of 1–5 mg.g^{-1} depending on the polymer (Table SI3). The powder was first diluted by a factor of 10 (powder 2, Table SI3), and 5 following external standards were obtained by further dilution (Table SI3). The standards were weighed in quartz tubes using a Micro Balance.

2.4. Py-GC-MS/MS analysis

Pyrolysis experiments were performed in a CDS Analytical Pyroprobe® Model 6150 (QUAD SERVICE, Achères, France) interfaced with a GC-MS/MS triple quadrupole TSQ® 9000 from Thermo Fisher Scientific (Villebon sur Yvette, France). The gas chromatography column was a TraceGOLD TG-5SilMS from Thermo Fisher Scientific. The optimized experimental parameters for Py-GC-MS/MS are summarized in Table SI4. Multiple reaction monitoring (MRM) optimizations for collision energy were obtained using Auto SRM 4.0 from Chromeleon®. MRM optimization was performed with the pure indicator compounds in liquid injection with a Thermo Scientific® AI/AS 1310 autosampler. There was an exception for the PP second indicator compound, for which the diastereoisomers of the 2,4,6,8-tetramethyl-1-undeceneseries (TeMC11) were not easily commercially available; thus, the optimization was performed from the pyrolysis of PP. The MS acquisition parameters are listed in Tables SI5 and SI6. The confirmation/quantification ratios were first established based on the chromatographic peaks after liquid injection and compared to those in the pyrolysis injection mode (Table SI5 and SI6). Chromatographic peaks were integrated using the Cobra detection algorithm from the Chromeleon® 7.2.8 software. For the pyrolysis, approximately 2 mg of external standards or sample was weighed in a quartz tube (ref 6201–3004, QUAD SERVICE, Achères, France) on a Sartorius Micro Balance. Then, online derivatization was performed with 5 μL of aqueous TMAH solution (25 wt%), which was directly spiked inside the pyrolysis tubes using a microsyringe (VWR, Pennsylvania, USA). The limits of detection and quantification (LOD and LOQ respectively) were defined with the classical criteria:

$$LOD = \overline{blank} + 3 \times (standard \quad deviation \quad Procedural \quad blank)$$

$$LOQ = \overline{blank} + 10 \times (standard \quad deviation \quad Procedrual \quad blank)$$

A compound was determined if the specific retention time deviation was less than 0.1 min and the ratio Tc/Tq deviation was less than ± 30% compared to the standards.

2.5. Sample preparation

Several bottles of mineral water purchased from the closest supermarket (Brand Eco +® 1.5 L from E.Leclerc) were filtered to obtain a total filtered volume of 20 L. The bottles made in PET were made of pristine polymer but it was indicated that the bottles were reusable, they were with a cap in PP. Filtrations were achieved using a Masterflex® IP33 Digital LED Variable-Speed Pump Drive from Cole-Parmer France, associated with a Masterflex® silicone tubing (Platinum) L/S® [24] (Cole-Parmer France) and an inox 1209 In-Line filter holder 25 mm from Pall Corporation (State of New York, USA). The tubing and filter holder unit limited the air exchanges and avoided any atmospheric deposition onto the glass fiber filter. Water filtration was performed on pre-calcined and weighed glass microfiber filters. For negative control we used MilliQ

water that was filter on calcined glass fiber filters in closed calcined glass unit. This water was stored in calcined glass bottles. The negative controls consisted of filtering this prepared with the exact same protocol used for the sample. After the water filtration, the filters from the sample and negative control were dried at 30 °C for 24 h in a closed glass petri dish, weighed and cryo-ground. Possible milling contamination was evaluated by grinding a calcined filter. In total, 6 replicates of cryo-ground filters, sample and negative control were analyzed. To consider the Py-GC-MS/MS signal intensity deviation, all external calibration standards and samples were analyzed in the same sequence on the same day.

3. Results and discussion

The method was developed for the most commonly used polymers: PMMA, PP, PE, PET, PS and PC. This is a common selection among the published Py-GC-MS developments [12]. The present study is not dedicated to investigating the matrix effect or polymer weathering impact on the pyrolytic response; these important aspects will be discussed in future work. The method development was conducted with an external calibration and applied to measure the polymer content in bottled water, where there should be no matrix interferences, and the present polymer certainly resulted from the manufacturing processes not weathered.

3.1. Indicator compound selection

The selection of indicator compounds for quantification was recently argued in a critical review, and it is consensual for most polymers (Table SI5) [12]. In addition to the detection of one indicator compound (I_1), it was recently proposed to select a second one (I_2) when it is possible to record their ratios (I_2/I_1) as additional validation criteria [2]. For PE, PP and PS, as several decomposition products were formed in important proportions, a second indicator compound was recorded, and the ratio (I_2/I_1) was used as an additional validation criterion (Table SI6).

For PE, many options remain open in terms of indicator compound selection [12]. The PE pyrolysis yields several hundred different hydrocarbons: linear or branched and containing 0–2 C-C double bound. The large number of peaks with relatively equal intensity suggests that the pyrolysis mechanism started with random scission. The pyrograms show a suite of equally spaced multiplets [25], which are often referred to as triplets considering the three most intense peaks. The triplet is successively composed of a terminal n-alkadiene (also called α,ω-alkadienes, CnD) followed by a terminal n-alkene (CnE) and an n-alkane (CnA). The second peak shows the highest response. CnE and CnA are not specific to the PE pyrolysis because natural organic matter pyrolysis produces these molecules, whereas CnD was identified to be more specific to PE pyrolysis [26]. CnD was formed in a much lower amount than the mono- or unsaturated congeners, and for the detection limit constraints, it was often proposed to monitor the mono unsaturated congeners but in counterpart with an intensive sample purification to avoid matrix interferences [20,21,27]. The higher sensitivity of the MS/MS detection allowed us to select the indicator compounds among the α,ω-alkadienes; congeners with 14 and 15 carbon atoms (C14D and C15D) were selected because they were the most intense and well-resolved peaks (Tables SI5 and SI6). The PP pyrolysis generates branched-chain hydrocarbons with a predominantly unsaturated structure. The selected indicator compounds are the two most intense peaks: 2,4-dimethylhept-1-ene (DMC7) and the most abundant diastereoisomer among the 2,4,6,8-tetramethyl-1-undecene series (TeMC11).

3.2. Instrument method development and MS/MS optimization

Working with pyrolysis, typically 1–2 mg of sample is weighed and introduced into the pyrolysis chamber. The repeated introduction of a solid sample is susceptible to larger experimental uncertainties than an automated liquid injection in the GC/MS system. Nonetheless, analytical pyrolysis later instrumental developments allowed us to provide a stable signal with a relative standard deviation (RSD) of 10–15% without internal standard corrections [28,29]' and good correlation values were presented for the calibration curves [2,28]. Using a simple quadrupole and working with traditional polymers, Fischer et al. [20,21], for example, provided external calibration between 0.4 and 1070 μg. The lowest point of the calibration was a consequence of the limit of the precision of the scale and the author explained that at this concentration the signal to noise ratio was important. Ribeiro et al. [2] or Okoffo et al. [18] analyzing microplastic in seafood tissues or in biosolid respectively, worked with calibration curves linear in the range 0.02–10 μg. These two studies presented low limit of quantification after sample extraction containing a step of pressurized liquid extraction from 0.07 to 24.3 μg.g^{-1} tissue [2] or from 0.03 to 0.37 μg.g^{-1} [18]. External standards in this range were carefully prepared by solid dilution in an inert matrix to provide good homogeneity (Table SI3). It was recently discussed that the solid diluent could act as a catalyst in the pyrolysis of some polymers, favoring the formation of different pyrolytic indicator compounds and thus impacting the quantification [30]. The authors showed that deactivated silica was very promising solid [30]. Here we have opted to used cryo-milled glass fiber filters because during sample preparation the sample (here bottled water) was filtered on glass fiber to collect and transfer the plastic particles to the pyrolysis chamber. The external calibration is then prepared in the exact same solid matrix as the sample. Briefly, we added a given amount of the initial powder to cryo-milled and calcined glass fiber filters. The mixture was again homogenized by cryo-milling because simple shaking was not sufficient enough. The homogeneity of the powder was controlled by repeated injection in Py-GC-MS/MS. We particularly recommend strictly restricting the amount of introduced polymer to the nanogram range to prevent source fouling or possible deterioration of the analyzer. Often, sample preparation consists in digestion and/or density separation; the last step of the sample preparation can be a filtration. The filter is first, a mean to collect and transfer the particles to the pyrolysis chamber but also a dilution media. Dilution factor that can be adjusted by the diameter and thickness of the glass fiber filter. After the homogenization steps have been optimized, the measured RSD over 6 replicates was 6–25% in the concentration range of 90–460 μg.g^{-1}, depending on the polymer.

The source transfer line and injector temperatures were optimized (Table SI4). The pyrolysis temperature was optimized by Hermabessierre et al. for PE, PC and PET [31]. We examined the pyrolysis temperature effect for the six selected polymers at 550–750 °C with standard calibration powder number 2 (Table SI3). The PE response was the faintest due to the selection of CnD as an indicator compound, which was considered when selecting the optimized pyrolysis temperature of 600 °C (Fig. SI1).

Since polymer pyrolysis generates a large number of molecules, pyrograms are very complex. We ensured that the detection and attribution of every indicator compound was free of interferences. To do so, the MS/MS detection parameters were optimized in liquid injection using the pure molecules as standards (Table SI2). The MRM responses were compared to those obtained after pyrolysis with the polymers alone or in mixture. After the GC condition optimization, we ensured that for all indicator compounds considered, there was less than 10% variation in the ion transition confirmation to quantification ratios (Tc/Tq) between GC-MS/MS and Py-GC-MS/MS (Table SI5). The particular case of PP is discussed in detail in the next section.

For PMMA, PET and PC detection, the use of TMAH as a methyl agent was necessary. According to Fischer et al., the use of TMAH does not affect the detection of other polymers [21]; this was verified under the present analytical conditions. To reduce the noise of the measure, we recommend the use of TMAH in crystals and the preparation of a solution at 25 wt% in ultra-pure water that was filtered on 0.1- μm PTFE Omnipore® membranes (47-mm diameter, Sigma—Aldrich) instead of

using a commercial solution. In the full scan, we observe that DMC7 systematically co-eluted with a substance, which we attributed to be a product of the decomposition of TMAH (mass spectra of the substance in Fig. SI2). Full separation was not achieved regardless of the tested GC conditions (temperature program, length of the column; data not shown). In MRM, DMC7 is not altered with the optimized transition, but we recommend caution in the SIM mode. DMC7 monitoring (ions at *m/z* 70 and 126) shows an alteration of the ratio if PP was analyzed pure diluted in glass fiber filter (ratio 12%) or in the standard mixture with TMAH (ratio 20%, data not shown).

3.3. Particular case of the hydrocarbon mass spectra

PE and PP are the most frequently detected polymers in the environment. They decompose into hydrocarbons that are not easily detected in mass spectrometry, so it is important to detail their responses. Straight-chain alkane molecular ions are usually weak. The molecular ions of the unsaturated derivatives are slightly more intense. It can be interesting to investigate lower collision energy, for example 30 eV, in order to enhance the signal of the hydrocarbon molecular ions. In the present study, the bottled waters tested present a simple matrix and the gain in selectivity working at lower collision energy and monitoring higher *m/z* ions was not significant (data not shown). For alkanes, the base peak in the mass spectra is usually at *m/z* 57 and corresponds to the C_4H_9 carbocation; it is surrounded by other smaller peaks due to the hydrogen atom rearrangement. The groups are separated by 14 at. mass units, which result from the loss of radical CH_2 (Fig. 1). For alkanes, the larger peak in the multiplets corresponds to the molecular formula $C_mH_{2\,m+1}$. With the same reasoning, the mass spectra of alkenes and α,ω-alkadienes contain carbocations at $C_mH_{2\,m-1}$ and $C_mH_{2\,m-2,}$ respectively (Fig. 1b and c). The base peak corresponds to the carbocation with m= 4; the exponential decay of the longer carbocations indicates a linear hydrocarbon. Prominent peaks with longer carbocations are typical for branched congeners (Fig. SI3 shows an example with alkene).

To summarize, among hydrocarbons, both structural isomers and congeners with distinct levels of unsaturation have common ions (Fig. 1). In addition, the use of high-resolution GC revealed the complexity of the mixture of a pyrolyzate. For example, in the case of PE, more than 140 different molecules were identified for congeners with 8 carbon atoms. Evidently, the use of classical GC does not fully separate the isomers [25].

Fig. 2 illustrates the response of the standard mixture magnified in the region of PE congeners with 13 carbon atoms in full scan, single ion monitoring and multiple reaction monitoring mode. The pyrogram is complex and PE indicator compound (the alkadiene) was surrounded by many peaks. The mass spectra of the peaks obtained from the full scan show co-eluting substances (Table SI7). We observed here that the peak ratios in SIM or MRM mode for the pure polymer or in the standard mixture were not modified (Table SI7). In the premises of microplastic analysis by Py-GC-MS the use of ratios was not systematically adopted to validate the detection of the peaks [20,21,26,27]. In SIM mode, several ions were more recently monitored [2,18]. As it was already reported in SIM mode, some ratios can be altered in a complex sample [32] so we recommend to use these criteria. As an additional validation step, we have analyzed the pure substances in liquid injection and made sure the ratios were the same to the pyrograms. Finally, the signal to noise ratio in MS/MS were superior to SIM experiment (Fig. 2).

3.4. PE and PP possible interferences

We recommend paying particular attention to the PE and PP interferences during method development, since all degradation products are hydrocarbons, and some indicator compounds present relatively similar Kovats retention indices. This was investigated with PE and PP mixtures in an inert matrix in proportions of PE/PP: 3/1; 1/1: and 1/3. The ratio Tc/Tq for CnD was recorded (Fig. 3). Interestingly, there was a linear correlation between Tc/Tq and the diene length. With n = 16, the introduction of increasing amounts of PP showed an anomaly. Some PP

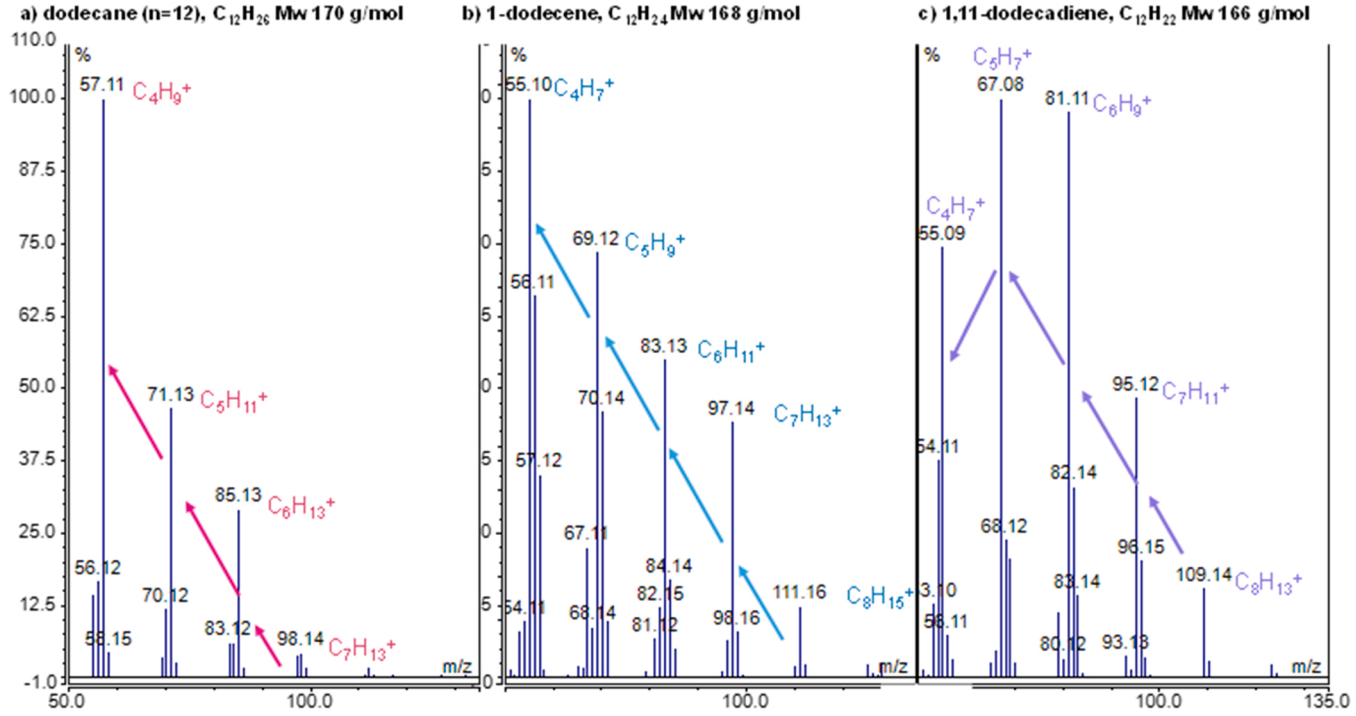

Fig. 1. Mass spectra of a) alkane, b) alkene and c) α,ω-alkadiene with n = 12. The arrow represents a loss of CH_2. The formula in bold character on top of each cluster corresponds to the most intense peak. For alkanes, the base peak is at *m/z* 57 and corresponds to the C_4H_9 carbocation; for n-alkenes, it is at *m/z* 55 and corresponds to C_4H_7; for α,ω-alkadienes, the base peak is at *m/z* 67 (the C_5H_7), but the ion *m/z* 55 is also intense. The 3 hydrocarbons present distinct degrees of unsaturation but nonetheless have many ions in common.

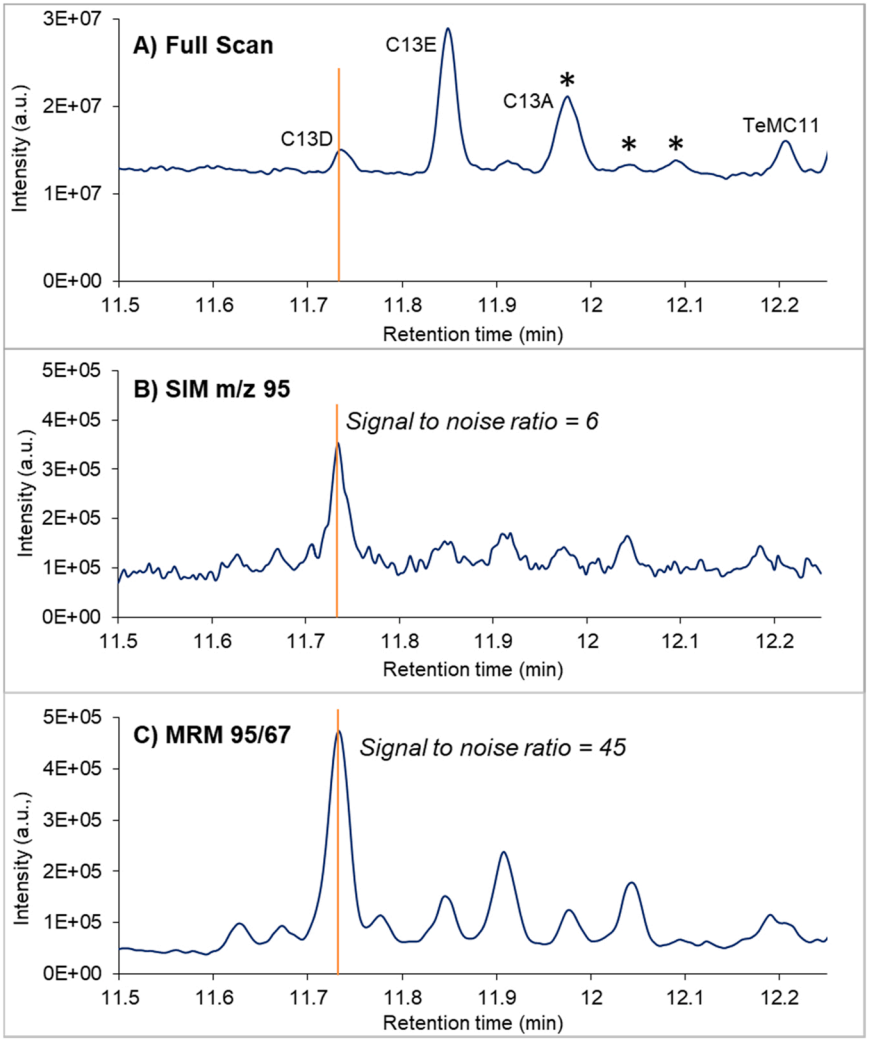

Fig. 2. A) Total ion current in full scan (TIC) of a mixture of 6 pyrolyzed polymers. The triplet specific to PE pyrolysis (at 700 ng) is presented, which is composed of the three congeners α,ω-alkadiene, n-alkene and n-alkane (C13D marked with an orange line, C13E and C13A). The peak labeled TeMC11 resulted from the PP pyrolysis. The peaks marked with a star were identified as the result of a mixture of co-eluting molecules after an examination of their mass spectra in the full scan. B) Single ion monitoring and C) Multiple reaction monitoring.

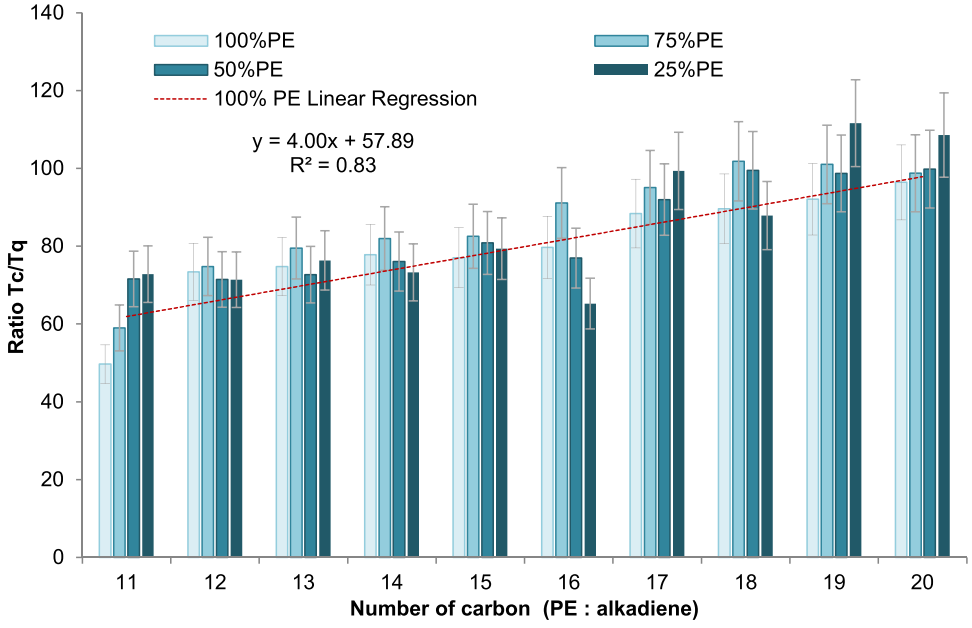

Fig. 3. Recording of the ion transitions Tc/Tq (*m/z* 109 >67 and 95 >67) when pyrolyzing a mixture of PE and PP with PE/PP ratios of 3/1, 1/1: and 1/3. for CnD.

decomposition products were co-eluting with this congener under the chromatographic conditions. Similar interactions were recorded with CnA and CnE (Fig. SI4). During method development, it is recommended to ensure that such interferences do not occur with the selected indicator compounds.

As previously mentioned, the MRM response of the indicator compounds was recorded with pure standards in liquid injection with the exception of TeMC11, which was not easily commercially available. Thus, it was important to pay particular attention to this peak and verify that there was no coelution. The peak was identified using its Kovats retention index (data from PubChem® for a standard nonpolar column), and its attribution was confirmed by comparing the mass spectra of the peak to the literature [33,34]. We ensured that the mass spectra of this peak and the relative proportion of the major ions did not change when PP was pyrolyzed alone or in mixture with other polymers.

The ratio I_2/I_1 was determined for PS, PE and PP. For PE, the ratio was remarkably stable over the entire study, injected alone or in mixture with other polymers (RSD 8%). For PP, the ratio was also stable (RSD 12%). In addition to the selected polymer to produce the external standards, other PP references were tested, and the ratio was consistent (homo or copolymers). In SIM mode, the monitoring DMC7 (*m/z* 70 and 126) and TeMC11 (*m/z* 111 and 83), the ratios were not altered by the presence of PE. For PS, there was more variation in the ratio (28%); this result was not rationalized.

3.5. External standard calibration and limit of quantification

The method was conducted with external calibration. The use of internal standard calibration was described for PS. This isotopic analog is commercially available; since PS is soluble in common solvent at room temperature, spiking is easy to repeat [28,35]. Since the isotopic analogs for the other polymers were not commercially available, we opted for external calibration. The R^2 values were 0.92–0.98 depending on the selected polymer (Table 1 and Fig. SI5) and highlighted a satisfactory correlation signal to the polymer amount.

The limits of MS/MS performances (analytical sensitivity) were not reached in this method development because at the lowest calibration points, the signal-to-noise ratios exceeded 10 for all considered indicator compounds. The analytical sensitivity was much lower than the LOQ and LOD. The LOD and LOQ were higher because of cross-contamination even if we pay particular attention to limiting it. There was a constant residual signal with the concentration point zero. The LOQ and LOD were in the range of nanograms per liter (as listed in Table SI8).

3.6. Application to the bottled water analysis

To apply this newly developed method, the polymer content in bottled water was determined. We selected this simply sample because it was reasonable to assume that there would be no matrix interferences, the present microplastics would certainly come from the manufacturing processes, and they consequently did not undergo weathering. We did not investigate these two aspects, but matrix interference [14,36] and polymer weathering [37,38] were reported to impact the polymer pyrolytic response.

After filtering 20 L of bottled water through a a GF/F glass fiber filter, cryo-grinding and analyzing the sample using Py-GC-MS/MS, we only determined the PET content. The other polymer concentrations were below the LOD (details of the LOQ levels are shown in Table SI8). The PET concentration in mineral water was measured at 42 ± 20 $ng.L^{-1}$. The concentration presented after 6 consequent analyses of the sample presented an important standard deviation of 50%. Two values were particularly high compared to the others, if we remove these values the standard deviation drops to 13% (n = 4), the concentration was thus determined at 28 ng/L (Table SI9). The outliers are certainly the result of air contamination while the sample remained on the autosampler module (a couples of hours).

The microplastic content in bottled water has been mainly determined using micro-Fourier transform infrared spectroscopy (μ-FTIR) [3,39] or micro-Raman spectroscopy [40,41]. Both techniques exhibited particle size limitations and did not provide the mass concentrations. For example, Ossmann et al. [40] found an average concentration of 2649 (RSD ± 2857) $particles.L^{-1}$ with 53.6% of the particles under a size of 1.5 μm and 44.7% in the range of 1.5–5.0 μm [40]. Polymer type ratio showed that 78% of the detected microplastics were PET, and the remainder was defined as olefins. We converted these results to mass concentration by assuming that the particles were spherical with a mean radius of 1.5 μm and using the known density of the specific polymer. We found a theoretical mass concentration of 2.62 $ng.L^{-1}$ for PET and 0.23 $ng.L^{-1}$ for olefins. With a radius of 5 μm, the PET concentration was 30 times higher (Table SI10). This result illustrates that the particle size is the major parameter that drives the variation in mass concentration. The determined PET concentration here was within the range given by Obmann et al. (0–81 $ng.L^{-1}$) [40].

Since Py-GC-MS/MS does not provide any information about particle size or number of particles, the obtained data here were converted the other way: 28 ng/L is estimated to correspond to 12000 and 320 $particles.L^{-1}$ using mean particles diamaters of 1.5 μm and 5 μm respectively. These kinds of calculations need to be treated with lot of care and are recommendable for rough comparison only. The conversion between mass and number of particles, and vice versa, allows us to concluded that studies using spectroscopic measurements [40] and the one presented here leads to the same range of concentrations.

3.7. Use of MS/MS requirements

Facing the tremendous complexity of a pyrogram, the accuracy of TOF-MS [24] or the selectivity of MS/MS drastically improves the performance of Py-GC-MS [17], as demonstrated here. These types of mass spectrometers have not been extensively tested with pyrolysis, certainly because the cost of purchase is limiting compared to simple quadrupole. The reason may be that a routine analysis using a simple quadrupole is sufficiently complex. The use of high-performance spectrometers requires highly specialized personnel and an important time implication for their maintenance. Pyrolysis is known to induce source fouling and column bleeding, so the signal quality must be monitored. We very regularly maintained the instrument. For example, the PET indicator

Table 1
Listing of calibration data for the investigated polymer and analytical limit. As a comparison to Py-GC-MS performances, analytical limits with an external calibration were reported [20]. In this study. it was specified that the limit of the method was the precision of the balance. Similarly, limits were later reported down to 500 ng and with the use of dissolved PS the LOD reached 30 ng for this polymer [21]. Finally in studies dedicated to the monitoring microplastic content in seafood the calibration curves were linear in the range 0.02–10 μg and the LOQ were from 0.07 to 24.3 $μg.g^{-1}$ tissue [2]. In biosolids the LOQ were between 0.03 and 0.37 $μg.g^{-1}$ [18].

Polymer	(I_1)	N	Calibration functions	R^2	Analytical limit (ng)	Reported limit of quantifications
PMMA	MeMeta	16	y = 3190.7x - 50154	0.9398	20	< 0.4 μg
PP	DMC7	15	y = 2702.8x + 9264.9	0.9470	20	< 0.6 μg
PE	C14D	16	y = 16.669x – 122.49	0.9873	70	< 50 μg
PET	DMeTPh	14	y = 11968x - 148766	0.9307	15	< 5 μg
PC	BPAMe	16	y = 112187x - 344480	0.9248	15	> 2.7 μg
PS	SSS	14	y = 3671.1x - 74477	0.9587	30	> 1.5 μg

compound peak broadening rapidly occurred and was solved with a maintenance of the GC column. Nonetheless, the use of high-performance spectrometers offers many promising perspectives, such as the development of high-throughput sample analysis, which is an important step toward the achievement of risk assessment studies.

4. Conclusion

In conclusion, the first goal of this study was to demonstrate the important improvements provided by using MS/MS. PP and PE were used to illustrate the unequivocal attribution of their indicator compounds using MRM experiments. The second aspect is the gain in detection limits, which reached the ng/L range, with MS/MS. Even if we took great care to control cross contamination, there was still polymer traces in the procedural blank. The limit of the study was the control of the cross contamination and not the performances of the mass spectrometer. Finally, the use of isotopic analogs to develop the internal standards will drastically improve the precision of the measure but is challenging [35]. Some aspects should be investigated to provide a robust method in complex samples. For matrix interferences, there is a balance between reducing the purification steps and controlling the matrix interferences [2,18]. Weathering also impacts the pyrolytic response of polymers, which must be addressed to provide a method to estimate the uncertainties of the measure [36,38].

Funding sources

This work was supported by the ANR (Agence Nationale de la Recherche) PRC program through the PEPSEA project (ANR- 17-CE34-0008-05).

Author contributions

The manuscript was written with contributions of all authors. All authors have given approval to the final version of the manuscript.

Declaration of Competing Interest

The authors declare that they have no known competing financial interests or personal relationships that could have appeared to influence the work reported in this paper.

Data Availability

No data was used for the research described in the article.

Acknowledgments

We acknowledge Julien Gigault and Bruno Grassl for the vivid and passionate discussion about polymer pyrolysis.

Appendix A. Supporting information

Supplementary data associated with this article can be found in the online version at doi:10.1016/j.jaap.2023.105993.

References

[1] C. Rochman, Microplastics research - from sink to source, Science 360 (6384) (2018) 28–29.
[2] F. Ribeiro, E.D. Okoffo, J.W. O'Brien, S. Fraissinet-Tachet, S. O'Brien, M. Gallen, S. Samanipour, S. Kaserzon, J.F. Mueller, T. Galloway, K.V. Thomas, Quantitative analysis of selected plastics in high-commercial-value australian seafood by pyrolysis gas chromatography mass spectrometry (vol 54, pg 9408, 2020), Environ. Sci. Technol. 54 (20) (2020), 13364-13364.
[3] A.A. Koelmans, N. Hazimah Mohamed Nor, E. Hermsen, M. Kooi, S.M. Mintenig, J. De France, Microplastics in freshwaters and drinking water: critical review and assessment of data quality, Water Res. (2019) 410–422.
[4] R. Geyer, J. Jambeck, K. Lavender Law, Production, use, and fate of all plastics ever made, Sci. Adv. (7) (2017).
[5] J.R. Jambeck, R. Geyer, C. Wilcox, T.R. Siegler, M. Perryman, A. Andrady, R. Narayan, K.L. Law, Plastic waste inputs from land into the ocean, Science 347 (6223) (2015) 768–771.
[6] R.C. Thompson, Y. Olsen, R.P. Mitchell, A. Davis, S.J. Rowland, A.W.G. John, D. McGonigle, A.E. Russell, Lost at sea: where is all the plastic? Science 304 (5672) (2004), 838-838.
[7] A. ter Halle, L. Ladirat, M. Martignac, A.F. Mingotaud, O. Boyron, E. Perez, To what extent are microplastics from the open ocean weathered? Environ. Pollut. 227 (2017) 167–174.
[8] L. Rowenczyk, A. Dazzi, A. Deniset-Besseau, V. Beltran, D. Goudouneche, P. Wong-Wah-Chung, O. Boyron, M. George, P. Fabre, C. Roux, A.F. Mingotaud, A. ter Halle, Microstructure Characterization of Oceanic Polyethylene Debris, Environ. Sci. Technol. 54 (7) (2020) 4102–4109.
[9] C. Schwaferts, R. Niessner, M. Elsner, N.P. Ivleva, Methods for the analysis of submicrometer- and nanoplastic particles in the environment, Trends Anal. Chem. 112 (2019) 52–65.
[10] S. Primpke, C. Lorenez, R. Rascher-Friesenhausen, G. Gerdts, An automated approach for microplasticds analysis using focal plane array (FPA) FTIR microscopy and image analysis, Anal. Methods 9 (2017) 1499.
[11] W. Cowger, A. Gray, S.H. Christiansen, H. DeFrond, A.D. Deshpande, L. Hemabessiere, E. Lee, L. Mill, K. Munno, B.E. Ossmann, M. Pittroff, C. Rochman, G. Sarau, S. Tarby, S. Primpke, Critical review of processing and classification techniques for images and spectra in microplastic research, Appl. Spectrosc. 74 (9) (2020) 989–1010.
[12] N. Yakovenko, A. Carvalho, A. ter Halle, Emerging use thermo-analytical method coupled with mass spectrometry for the quantification of micro(nano)plastics in environmental samples, TrAC Trends Anal. Chem. 131 (2020), 115979.
[13] D. Fabbri, A.G. Rombola, I. Vassura, C. Torri, S. Franzellitti, M. Capolupo, E. Fabbri, Off-line analytical pyrolysis GC?MS to study the accumulation of polystyrene microparticles in exposed mussels, J. Anal. Appl. Pyrolysis 149 (2020).
[14] Y. Pico, D. Barcelo, Pyrolysis gas chromatography-mass spectrometry in environmental analysis: focus on organic matter and microplastics, Trac-Trend Anal. Chem. 130 (2020).
[15] A. ter Halle, L. Jeanneau, M. Martignac, E. Jarde, B. Pedrono, L. Brach, J. Gigault, Nanoplastic in the north atlantic subtropical gyre, Environ. Sci. Technol. 51 (23) (2017) 13689–13697.
[16] G.L. Sullivan, J.D. Gallardo, E.W. Jones, P.J. Hollliman, T.M. Watson, S. Sarp, Detection of trace sub-micron (nano) plastics in water samples using pyrolysis-gas chromatography time of flight mass spectrometry (PY-GCToF), Chemosphere 249 (2020).
[17] M. Albignac, J.F. Ghiglione, C. Labrune, A. ter Halle, Determination of the microplastic content in Mediterranean benthic macrofauna by pyrolysis-gas chromatography-tandem mass spectrometry, Mar. Pollut. Bull. 181 (2022), 113882.
[18] E.D. Okoffo, F. Ribeiro, J.W. O'Brien, S. O'Brien, B.J. Tscharke, M. Gallen, S. Samanipour, J.F. Mueller, K.V. Thomas, Identification and quantification of selected plastics in biosolids by pressurized liquid extraction combined with double-shot pyrolysis gas chromatography-mass spectrometry, Sci. Total Environ. 715 (2020).
[19] P. Eisentraut, E. Dumichen, A.S. Ruhl, M. Jekel, M. Albrecht, M. Gehde, U. Braun, Two birds with one stone-fast and simultaneous analysis of microplastics: microparticles derived from thermoplastics and tire wear, Environ. Sci. Tech. Let. 5 (10) (2018) 608–613.
[20] M. Fischer, B.M. Scholz-Bottcher, Simultaneous trace identification and quantification of common types of microplastics in environmental samples by pyrolysis-gas chromatography-mass spectrometry, Environ. Sci. Technol. 51 (9) (2017) 5052–5060.
[21] M. Fischer, B.M. Scholz-Bottcher, Microplastics analysis in environmental samples - recent pyrolysis-gas chromatography-mass spectrometry method improvements to increase the reliability of mass-related data, Anal. Methods 11 (18) (2019) 2489–2497.
[22] S. Primpke, M. Fischer, C. Lorenz, G. Gerdts, B.M. Scholz-Bottcher, Comparison of pyrolysis gas chromatography/mass spectrometry and hyperspectral FTIR imaging spectroscopy for the analysis of microplastics, Anal. Bioanal. Chem. 412 (30) (2020) 8283–8298.
[23] E. Duemichen, P. Eisentraut, M. Celina, U. Braun, Automated thermal extraction-desorption gas chromatography mass spectrometry: A multifunctional tool for comprehensive characterization of polymers and their degradation products, J. Chromatogr. A 1592 (2019) 133–142.
[24] G.F. Schirinzi, M. Llorca, R. Sero, E. Moyano, D. Barcelo, E. Abad, M. Farre, Trace analysis of polystyrene microplastics in natural waters, Chemosphere 236 (2019).
[25] L. Sojak, R. Kubinec, H. Jurdakova, E. Hajekova, M. Bajus, High resolution gas chromatographic-mass spectrometric analysis of polyethylene and polypropylene thermal cracking products, J. Anal. Appl. Pyrolysis 78 (2) (2007) 387–399.
[26] E. Dumichen, A.K. Barthel, U. Braun, C.G. Bannick, K. Brand, M. Jekel, R. Senz, Analysis of polyethylene microplastics in environmental samples, using a thermal decomposition method, Water Res. 85 (2015) 451–457.
[27] A. Gomiero, K.B. Oysaed, T. Agustsson, N. van Hoytema, T. van Thiel, F. Grati, First record of characterization, concentration and distribution of microplastics in coastal sediments of an urban fjord in south west Norway using a thermal degradation method, Chemosphere 227 (2019) 705–714.
[28] K.M. Unice, M.L. Kreider, J.M. Panko, Use of a deuterated internal standard with pyrolysis-GC/MS dimeric marker analysis to quantify tire tread particles in the environment, Int. J. Environ. Res. Public Health 9 (11) (2012) 4033–4055.

[29] G. Dierkes, T. Lauschke, S. Becher, H. Schumacher, C. Foeldi, T. Ternes, Quantification of microplastics in environmental samples via pressurized liquid extraction and pyrolysis-gas chromatography, Anal. Bioanal. Chem. 411 (26) (2019) 6959–6968.
[30] M. Matsueda, M. Mattonai, I. Iwai, A. Watanabe, N. Teramae, W. Robberson, H. Ohtani, Y.-M. Kim, C. Watanabe, Preparation and test of a reference mixture of eleven polymers with deactivated inorganic diluent for microplastics analysis by pyrolysis-GC–MS, J. Anal. Appl. Pyrolysis 154 (2021), 104993.
[31] L. Hermabessiere, C. Himber, B. Boricaud, M. Kazour, R. Amara, A.L. Cassone, M. Laurentie, I. Paul-Pont, P. Soudant, A. Dehaut, G. Duflos, Optimization, performance, and application of a pyrolysis-GC/MS method for the identification of microplastics, Anal. Bioanal. Chem. 410 (25) (2018) 6663–6676.
[32] E. Dumichen, P. Eisentraut, C.G. Bannick, A.K. Barthel, R. Senz, U. Braun, Fast identification of microplastics in complex environmental samples by a thermal degradation method, Chemosphere 174 (2017) 572–584.
[33] S. Tsuge, H. Othani, C. Watanabe, Pyrolysis-GC/MS Data book of synthetic polymers, Elsevier, 2011.
[34] C.C. Moldoneavu, Analytical pyrolysis of synthetic organic polymers (Elseveir ed.), Elsevier, 2005.
[35] T. Lauschke, G. Dierkes, P. Schweyen, T.A. Ternes, Evaluation of poly(styrene-d5) and poly(4-fluorostyrene) as internal standards for microplastics quantification by thermoanalytical methods, J. Anal. Appl. Pyrolysis 159 (2021).
[36] N. Bouzid, C. Anquetil, R. Dris, J. Gasperi, B. Tassin, S. Derenne, Quantification of microplastics by pyrolysis coupled with gas chromatography and mass spectrometry in sediments: challenges and implications, Microplastics 1 (2) (2022) 229–239.
[37] N.M. Ainali, D.N. Bikiaris, D.A. Lambropoulou, Aging effects on low- and high-density polyethylene, polypropylene and polystyrene under UV irradiation: an insight into decomposition mechanism by Py-GC/MS for microplastic analysis, J. Anal. Appl. Pyrolysis 158 (2021).
[38] T. Toapanta, E.D. Okoffo, S. Ede, S. O'Brien, S.D. Burrows, F. Ribeiro, M. Gallen, J. Colwell, A.K. Whittaker, S. Kaserzon, K.V. Thomas, Influence of surface oxidation on the quantification of polypropylene microplastics by pyrolysis gas chromatography mass spectrometry, Sci. Total Environ. 796 (2021).
[39] S.A. Mason, V.G. Welch, J. Neratko, Synthetic polymer contamination in bottled water, Front. Chem. 6 (2018).
[40] B.E. Ossmann, G. Sarau, H. Holtmannspotter, M. Pischetsrieder, S.H. Christiansen, W. Dicke, Small-sized microplastics and pigmented particles in bottled mineral water, Water Res. 141 (2018) 307–316.
[41] D. Schymanski, C. Goldbeck, H.U. Humpf, P. Furst, Analysis of microplastics in water by micro-Raman spectroscopy: release of plastic particles from different packaging into mineral water, Water Res. 129 (2018) 154–162.